

Kinematical data on early-type galaxies. I.^{*,**}

F. Simien and Ph. Prugniel

CRAL-Observatoire de Lyon (CNRS: UMR 142), F-69561 St-Genis-Laval Cedex, France

Received May 2; accepted August 21, 1996

Abstract. As part of an ongoing program on the main parameters of early-type galaxies, we have performed long-slit absorption spectroscopy on a sample of 21 ellipticals and S0s. We present determinations of the central velocity dispersion and, for 18 objects, velocity-dispersion profiles and rotation curves.

Key words: galaxies: elliptical & lenticular, cD — galaxies: kinematics and dynamics — galaxies: fundamental parameters

1. Introduction

The last decade has witnessed an almost explosive growth in the availability of global parameters on early-type galaxies. Photometric and kinematical data on large samples of objects, for example, have led to the discovery of the Fundamental Plane (hereafter FP): Faber et al. (1987), Djorgovski & Davis (1987). Since these pioneering works, many more observations have been carried out, either to complete statistically significant samples, or to get better measurements on parameters already available; it should be stressed, indeed, that several subtle physical effects related to the FP barely emerge from the measurement errors, and that their study requires the best possible data.

For the kinematics, the main parameter concerned is still the central velocity dispersion σ_0 , which accounts for most of the kinetic energy. It is clear from recent compilations (McElroy 1995; Prugniel & Simien 1996, hereafter PS96) that its availability is growing, and that its accuracy is improving.

Recent studies have shown that the role of the rotation, although hardly dominating in most early-type galaxies,

has nevertheless a statistical significance in the global scaling relations (Busarello et al. 1992; Prugniel & Simien 1994, hereafter PS94; Bender et al. 1994; D’Onofrio et al. 1995a; Prugniel & Simien 1995). The surveys of the literature show that measurements of the maximum rotation V_{\max} are available on a modest proportion of early-type galaxies for which σ_0 is known, although there has been many very recent contributions dealing with more than a dozen objects (e.g., Bender et al. 1994; Carollo & Danziger 1994; Fried & Illingworth 1994; Longo et al. 1994; PS94; D’Onofrio et al. 1995b; Fisher et al. 1995; Seifert & Scorza 1996).

In PS94 and PS96, we have started to present our measurements of σ_0 and V_{\max} , as part of the data we have used in our study on kinematical and stellar-population effects related to the FP. In this paper, we present the central velocity dispersion for 21 objects, and profiles of $\sigma(r)$ and $V(r)$ for 18 objects.

2. Sample and observations

The present sample gathers ellipticals between E0 and E4, together with S0s; it belongs to a larger sample for which the proportion of S0s had been deliberately enhanced in order to increase the bias toward large rotation velocities.

Most of these objects have a distance between $\simeq 15$ and $\simeq 30$ Mpc (for $H_0 = 75 \text{ km s}^{-1} \text{ Mpc}^{-1}$), and eight of them are at more than 55 Mpc. The absolute magnitudes are in the range $-21.7 < M_B < -18.0$.

Catalog elements are found in Table 1; here, the integrated magnitude, the absolute magnitude, and the effective radius of the galaxies are from Prugniel & Simien (1997; hereafter PS97). Knowledge of the orientation of the major axis is required for a meaningful measurement of the rotation velocity; care has been taken to search the literature for the most reliable value of its position angle (PA), and when we found evidence for a significant twist of the isophotes, we adopted a PA representative of the inner region where spectroscopic data could be obtained. Table 1 gives the reference for the PA determination.

Our kinematical observations have been secured at the 1.93-m telescope of the Observatoire de Haute-Provence,

Send offprint requests to: F. Simien (simien@obs.univ-lyon1.fr)

* Based on observations collected at the Observatoire de Haute-Provence.

** Table 4 is presented in electronic form only; Tables 3 and 4 are available from the CDS, Strasbourg (anonymous ftp to 130.79.128.5).

Table 1. Catalog elements

Object	Type	α_{1950}	δ_{1950}	v_{hel}	B_{T}	$-M_B$	r_e	ϵ	PA	ref.	σ_0	V_{max}
(1)	(2)	(3)	(4)	(5)	(6)	(7)	(8)	(9)	(10)	(11)	(12)	(13)
NGC 97	-5	00 19 52.7	29 28 06	4790	13.36	20.66	13.5	0.05	9	1	118 ± 32	... ± ...
NGC 383	-3	01 04 39.4	32 08 46	5096	12.06	21.70	54.1	0.30	141	1	258 ± 18	129 ± 35
NGC 430	-5	01 10 25.8	-00 31 02	5283	13.80	20.11	9.4	0.30	158	1	301 ± 14	... ± ...
NGC 499	-3	01 20 22.4	33 11 57	4375	12.96	20.75	15.0	0.23	82	4	237 ± 24	... ± ...
NGC 1199	-5	03 01 18.1	-15 48 31	2660	12.20	20.09	30.4	0.23	51	1	207 ± 11	... ± ...
NGC 1426	-5	03 40 38.0	-22 16 06	1412	12.22	19.35	25.6	0.37	105	1	152 ± 09	... ± ...
NGC 1461	-2	03 46 09.9	-16 32 38	1426	12.59	18.98	16.6	0.70	155	4	209 ± 15	140 ± 21
NGC 1713	-4	04 56 21.3	-00 33 57	4514	12.76	20.97	37.0	0.15	45	4	254 ± 26	... ± ...
NGC 2329	-3	07 05 21.7	48 41 48	5765	12.98	21.29	21.5	0.14	175	4	244 ± 19	99 ± 05
NGC 2332	-2	07 05 43.3	50 15 48	5808	13.85	21.08	...	0.33	60	4	... ± ± ...
NGC 2685	-2	08 51 41.2	58 55 30	881	11.94	19.06	30.1	0.53	38	4	103 ± 17	< 100 ± ...
NGC 2732	-2	09 06 52.8	79 23 33	1902	12.64	19.54	17.2	0.30	67	3,4	170 ± 18	126 ± 19
NGC 2768	-5	09 07 45.2	60 14 40	1334	10.74	20.86	61.2	0.36	95	4	193 ± 11	78 ± 34
NGC 3193	-5	10 15 39.5	22 08 45	1364	11.64	20.03	31.0	0.08	93	1	193 ± 14	80 ± 13
NGC 3818	-5	11 39 24.2	-05 52 43	1498	12.51	19.15	23.2	0.38	97	1	199 ± 10	114 ± 07
NGC 4434	-5	12 25 04.2	08 25 53	1063	13.03	17.98	12.9	0.09	33	1	118 ± 15	... ± ...
NGC 4476	-3	12 27 26.7	12 37 27	1931	13.00	18.01	14.8	0.34	29	2	82 ± 48	... ± ...
NGC 4478	-5	12 27 45.5	12 36 18	1417	12.23	18.78	11.9	0.18	133	1	143 ± 11	62 ± 05
NGC 7660	-5	23 23 20.3	26 45 13	5691	13.43	20.66	17.2	0.25	26	1	207 ± 38	... ± ...
NGC 7727	1	23 37 18.6	-12 34 14	1860	11.53	20.09	27.0	0.14	35	4	181 ± 10	... ± ...
UGC 3696	-5	07 05 36.9	48 42 58	6118	13.60	20.93	21.1	0.28	77	4	260 ± 26	... ± ...

*Notes:*Col. (2): morphological type (from the *LEDA* database);

Cols. (3), (4): coordinates;

Col. (5): v_{hel} , heliocentric radial velocity, in km s^{-1} (from *LEDA*);Col. (6): B_{T} , integrated blue magnitude, corrected for Galactic extinction and k term (from PS97);Col. (7): $-M_B$, absolute B magnitude (from PS97);Col. (8): r_e , effective radius (from PS97), in arcsec;Col. (9): ϵ , ellipticity;

Col. (10): PA, position angle of major axis, in degrees (North through East);

Col. (11): reference for ϵ and PA, 1 = Djorgovski (1985), 2 = Michard (1985), 3 = Michard & Marchal (1993), 4 = *LEDA*;Col. (12): σ_0 , central velocity dispersion available in the literature, from the compilation in PS96, in km s^{-1} ;Col. (13): V_{max} , maximum rotational velocity available in the literature, from the compilation in PS96, in km s^{-1} .

equipped with the *CARELEC* long-slit spectrograph¹ (Prugniel et al. 1992). The camera aperture ratio was $f/2.6$, and the receptor was a Tektronix with 512×512 pixels of $27 \mu\text{m}$, corresponding to a projected size of $1.2''$. The selected setup provided a wavelength range of $\approx 900 \text{ \AA}$ centered on Mg_b , with a FWHM resolution of 1.8 \AA per pixel (i.e., 104 km s^{-1} at $\lambda = 5200 \text{ \AA}$). The slit width, projected onto the plane of the sky, was $2.2''$.

In January 1995, a five-night observing run collected data on the major axis of our program galaxies. Typically, two 45-minute exposures were obtained for each object; this individual exposure time was considered long enough to ensure a sufficient S/N ratio on most galaxies, yet short enough to prevent the widening of the spectral lines due to flexures within the spectrograph. For NGC 2732 and

NGC 4478, spectra along the minor axis were also obtained. Each night, several template stars of types ranging between G8III and K2III were observed.

The atmospheric conditions were variable, with a seeing disk between $2.5''$ and $3.6''$ (FWHM) for most objects, but up to $\simeq 6''$ for four of them; with the exception of NGC 430, galaxies with $r_e < 10''$ were not observed when the seeing was poorer than $4''$. The log of the observations is given in Table 2.

3. Data reduction

3.1. Pre-processing

Standard procedures have been used, with the ESO-Midas reduction package, to flatfield the spectra (using exposures taken on the illuminated dome) and to transform the abscissae into wavelength (with calibration He- and Ne-lamp spectra); the calibration spectra taken before and after

¹ Details on the spectrograph, on the receptor, and information on the telescope itself are available on the WWW, at URL <http://www.obs-hp.fr>

Table 2. Log of observations

Object	date	PA	exp.	seeing
(1)	(2)	(3)	(4)	(5)
NGC 97	04.01.95	9	2 × 45	3.5
NGC 383	04.01.95	141	2 × 45	3.5
NGC 430	02.01.95	155	2 × 45	≈ 6
NGC 499	04.01.95	82	2 × 45	2.5
NGC 1199	05.01.95	48	2 × 45	2.2
NGC 1426	03.01.95	103	2 × 45	3.6
NGC 1461	07.01.95	155	2 × 45	2.5
NGC 1713	02.01.95	45	2 × 45	≈ 6
NGC 2329	03.01.95	175	2 × 45	3.5
NGC 2332	03.01.95	60	2 × 45	3.3
NGC 2685	04.01.95	38	2 × 45	3.5
NGC 2732	07.01.95	67	1 × 45	2.5
NGC 2732	07.01.95	157	1 × 45	2.5
NGC 2768	04.01.95	95	2 × 45	3.5
NGC 3193	02.01.95	92	1 × 45	≈ 6
NGC 3818	04.01.95	97	1 × 45	3.5
NGC 4434	03.01.95	32	1 × 45	2.8
NGC 4476	02.01.95	25	2 × 45	≈ 6
NGC 4478	07.01.95	140	2 × 60	2.5
NGC 4478	07.01.95	50	2 × 60	2.5
NGC 7660	02.01.95	35	1 × 45	≈ 6
NGC 7727	04.01.95	35	2 × 45	3.5
UGC 3696	03.01.95	77	2 × 45	2.8

Notes:

Col. (3): PA, position angle of slit, in degrees;
 Col. (4): exp., number of spectra and exposure time in minutes;
 Col. (5): seeing, FWHM in arcsec.

each long exposure on a galaxy were checked for possible wavelength shift by a cross-correlation routine, and the result was considered acceptable for a shift smaller than a third of a pixel.

For the determination of the galaxy center, we have calculated the photometric profile by averaging the pixel luminosities in the direction of the dispersion, and we have adopted the position provided by a gaussian fitting on a range of $\simeq 10$ pixels ($\simeq 12''$) around the brightest point. This is close to the photometric center but, obviously, this choice involves a part of arbitrariness, since there is evidence for a slight asymmetry in some objects.

3.2. Measurement of kinematical parameters

We have used a Fourier-Fitting technique similar to that of Franx et al. (1989) for the simultaneous determination of the velocity dispersion $\sigma(r)$, and the rotational velocity $V(r)$ at distance r from the center; also determined was a parameter $\gamma(r)$ related to the absorption-line contrast with respect to an approximation of the continuum, represented by a third-order polynomial fitting to the spectrum.

Table 3. Kinematical results

Object	v_{hel}	σ_0	V_{max}	r_{max}
(1)	(2)	(3)	(4)	(5)
NGC 97	4766 ± 13	188 ± 15	29 ± 14	10
NGC 383	5090 ± 13	280 ± 22	103 ± 23	15
NGC 430	5268 ± 21	229 ± 24*	... ±
NGC 499	4363 ± 18	254 ± 16	... ±
NGC 1199	2701 ± 13	194 ± 13	52 ± 16	16
NGC 1426	1450 ± 13	162 ± 14	114 ± 19	20
NGC 1461	1467 ± 13	216 ± 13	165 ± 15	38
NGC 1713	4438 ± 22	194 ± 21	... ±
NGC 2329	5791 ± 18	246 ± 18	87 ± 27	11
NGC 2332	5806 ± 16	259 ± 16	< 15 ±
NGC 2685	883 ± 11	103 ± 12	100 ± 07	31
NGC 2732	1996 ± 13	168 ± 12	147 ± 10	30
NGC 2768	1385 ± 13	197 ± 13	182 ± 17	60
NGC 3193	1399 ± 14	213 ± 15	< 20 ±
NGC 3818	1701 ± 16	198 ± 16	91 ± 15	13
NGC 4434	1070 ± 13	121 ± 16	41 ± 16	15
NGC 4476	1978 ± 12	65 ± 13	36 ± 11	10
NGC 4478	1381 ± 13	156 ± 12	54 ± 10	20
NGC 7660	5670 ± 25	276 ± 21	130 ± 27	12
NGC 7727	1855 ± 13	220 ± 13	116 ± 20	16
UGC 3696	6135 ± 18	248 ± 19	154 ± 27	12

Notes:

Col. (2): v_{hel} , heliocentric radial velocity, in km s^{-1} ;
 Col. (3): σ_0 , central velocity dispersion, in km s^{-1} ;
 Col. (4): V_{max} , maximum rotation velocity, in km s^{-1} ;
 Col. (5): r_{max} , the radius at which V_{max} has been measured, in arcsec;
 (*): σ_0 is uncertain due to bad seeing conditions.

For the outer, faint spectra of a galaxy, removing the cosmic-ray hits was done by a median filtering perpendicularly to the dispersion. For the inner spectra, for which this procedure would have degraded the spatial resolution, we relied instead on a three-sigma clipping on the residuals between the galaxy spectrum and the (shifted and convolved) star spectrum: the V and σ parameters were actually determined by two successive steps, the first using the raw galaxy spectrum, and the second the spectrum with cosmic rays removed as explained.

In order to enhance the S/N ratio of outer spectra, adjacent lines were averaged: for a spectrum at radius r , a weight was assigned to the neighboring lines ($r \pm \delta r$) entering the average; for this weight, a gaussian fall-off as a function of δr was chosen, with a FWHM width between 0 and 3 pixels (0 and $3.5''$); the central spectrum was never averaged. The two successive spectra obtained at the same position angle were either co-added before running the Fourier-Fitting code, or processed independently; in the latter case, the σ and V profiles were combined. The two approaches have yielded very similar results.

For most galaxies, profiles of $\sigma(r)$ and the rotational velocity $V(r)$ were determined, and presented in Fig. 1; for

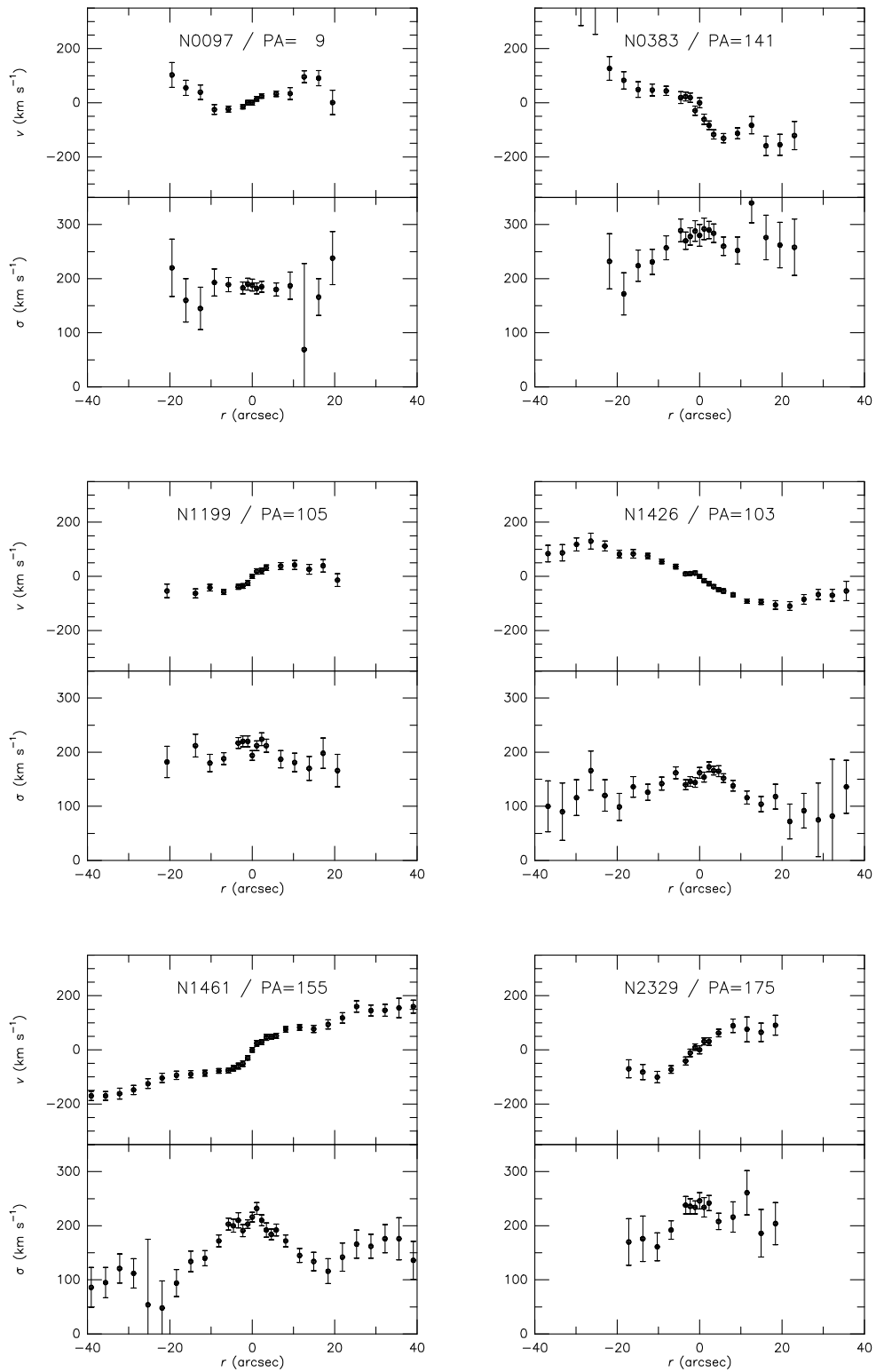


Fig. 1. Profiles of rotational velocities and velocity dispersions

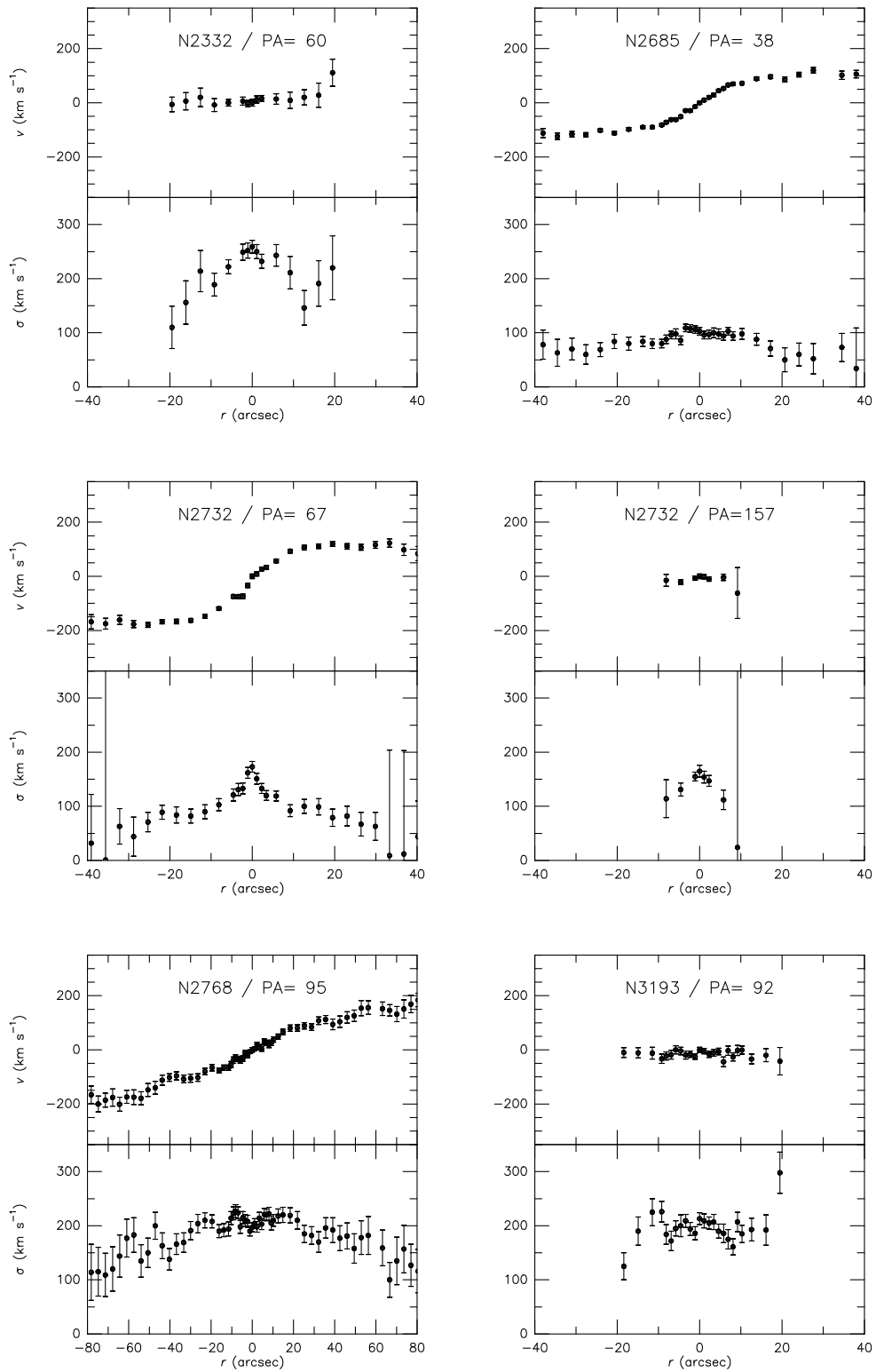


Fig. 1. continued

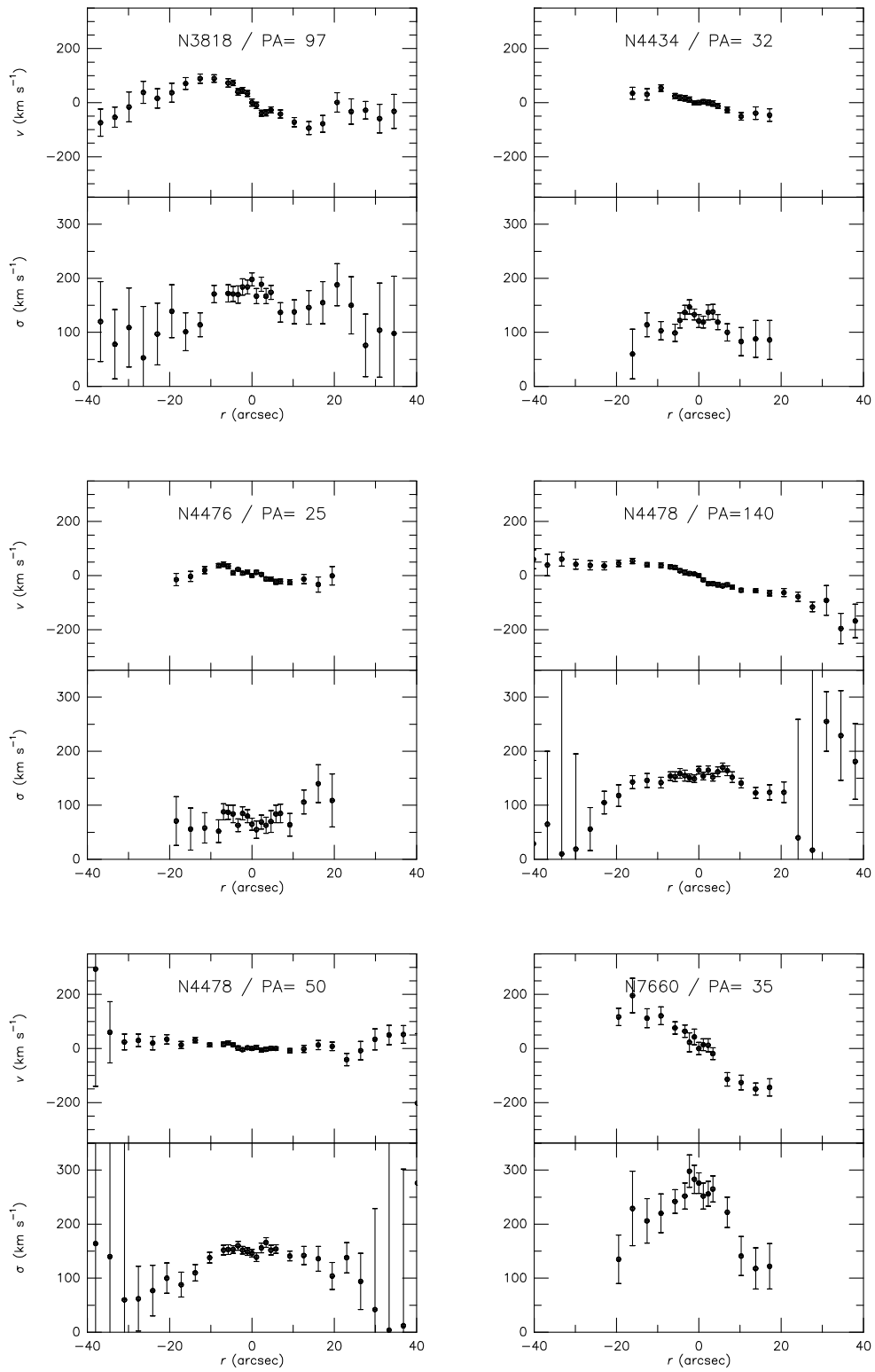


Fig. 1. continued

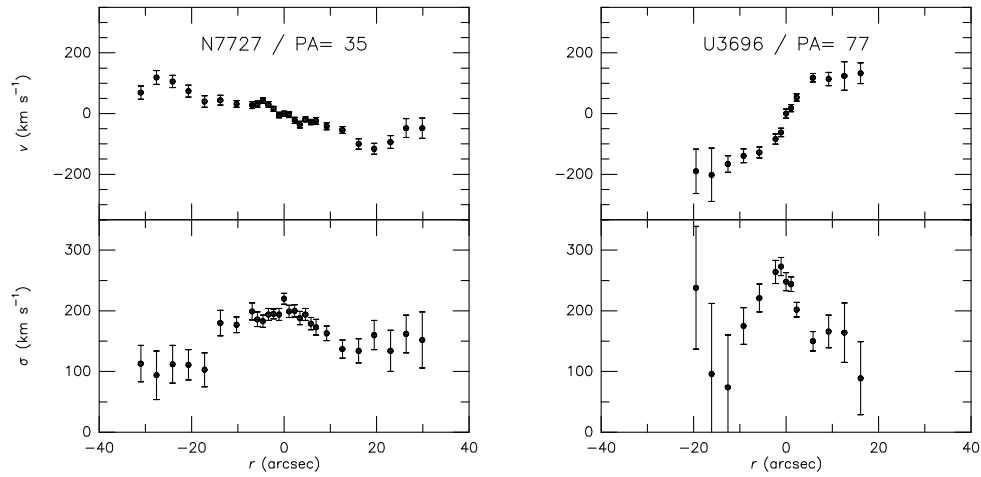


Fig. 1. continued

the latter, we adopted as the systemic velocity the radial velocity measured at $r = 0$. The determination of the maximum rotation V_{\max} was done as follows: on each semi-major axis, in a region of reliable measurements, a radius r_{\max} was determined, where the corresponding $V(r_{\max})$ was thought to represent the maximum rotation, and we adopted as V_{\max} the mean of these two values. We note that this definition bypasses the possible asymmetry of the rotation curve with respect to the adopted center, and it is likely to provide a fair approximation to the rotational kinetic energy.

Table 3 shows the values of the central velocity dispersion σ_0 and, except for three objects for which the spectra were faint, the value of $V(r_{\max})$, together with the mean of the two determinations of r_{\max} . For the two galaxies with major- and minor-axis observations, Table 3 gives as σ_0 the average of the two determinations. Table 4, which is available in electronic form only, gathers the V and σ profiles.

4. Discussion

We have presented kinematical data for 21 early-type galaxies. Among the 18 objects for which we have measured V_{\max} , nine had no previously published value; and NGC 2332 had no previous determinations of σ_0 . For most of them, our profiles extend to more than one r_e .

Comparisons with data from the literature lead to the following two comments:

- for a couple of galaxies, we note significant differences in σ_0 , but the overall agreement is good: for 20 objects, our dispersions are on average within 12% of the others. For these objects, the mean of the residuals R_{FP} with respect to the Fundamental Plane, (as calculated by PS96, but with no rotation and no stellar-population effects included), is slightly reduced, from -0.06 down to -0.03 , when replacing the literature

values by our measurements; and the scatter in R_{FP} is also marginally reduced, from 0.22 (rms) to 0.19. We are thus confident in the overall reliability of our dispersions.

- there is evidence, from the nine galaxies with previous V_{\max} measurements, that the discrepancy is much larger for the rotation than for the dispersion; this may come from two effects, a difference in the adopted PA, and a different distance r for the determination: the case of NGC 2768 is revealing, our new determination corresponding to the second plateau in the rotation curve; this justifies the indication of r_{\max} in Table 3.

Acknowledgements. We are indebted to the telescope operators at the Observatoire de Haute-Provence for their help in collecting the data. We thank the referee, G. Busarello, for his comments. We have made use of the Lyon-Meudon Extragalactic Database supplied by the *LEDA* team.

References

- Bender R., Saglia R.P., Gerhard O.E., 1994, MNRAS 269, 785
 Busarello G., Longo G., Feoli A., 1992, A&A 262, 52
 Carollo C.M., Danziger I.J., 1994, MNRAS 270, 523
 Djorgovski S., 1985, PhD thesis, Univ. of California, Berkeley
 Djorgovski S., Davis M., 1987, ApJ 313, 59
 D’Onofrio M., Longo G., Capaccioli M., 1995a, in: Buzzoni A., Renzini A., Serrano G. (eds.) Fresh views of elliptical galaxies, ASPCS 86, 143
 D’Onofrio M., Zaggia S.R., Longo G., Caon N., Capaccioli M., 1995b, A&A 296, 319
 Faber S.M., Dressler A., Davies R.L., Burstein D., Lynden-Bell D., Terlevich R.J., Wegner G., 1987, in: Faber S.M. (ed.) Nearly Normal Galaxies. Springer, Berlin, p. 175
 Fisher D., Illingworth G.D., Franx M., 1995, ApJ 438, 539
 Franx M., Illingworth G., Heckman T., 1989, ApJ 344, 613
 Fried J.W., Illingworth G.D., 1994, AJ 107, 992
 Longo G., Zaggia S.R., Busarello G., Richter G., 1994, A&AS 105, 433

- McElroy D.B., 1995 *ApJS* 100, 105
Michard R., 1985, *A&AS* 59, 205
Michard R., Marchal J., 1993, *A&AS* 98, 29
Prugniel Ph., Rampazzo R., Simien F., 1992, *La lettre de l'OHP* No. 8, p. 1
Prugniel Ph., Simien F., 1994, *A&A* 281, L1 (PS94)
Prugniel Ph., Simien F., 1995, in: Buzzoni A., Renzini A., Serrano G. (eds.). *Fresh views of elliptical galaxies*, ASPCS 86, 151
Prugniel Ph., Simien F., 1996, *A&A* 309, 749 (PS96)
Prugniel Ph., Simien F., 1997, *A&A* (in press) (PS97)
Seifert W., Scorza C., 1996, *A&A* 310, 75